Published in final edited form as:
J Biomed Mater Res A. 2012 June ; 100(6): 1605–1614. doi:10.1002/jbm.a.34102.

Modulation of Gene Expression using Electrospun Scaffolds with Templated Architecture

A. Karchin, Ph.D.[1], **Y-N Wang, Ph.D.**[2], and **J.E. Sanders, Ph.D.**[1]

[1]Department of Bioengineering, Box 355061, University of Washington, Seattle, Washington 98195, USA

[2]Center for Medical and Industrial Ultrasound, Applied Physics Laboratory, University of Washington, Seattle, Washington 98195, USA

Abstract

The fabrication of biomimetic scaffolds is a critical component to fulfill the promise of functional tissue engineered materials. We describe herein a simple technique, based on printed circuit board manufacturing, to produce novel templates for electrospinning scaffolds for tissue engineering applications. This technique facilitates fabrication of electrospun scaffolds with templated architecture, which we defined as a scaffold's bulk mechanical properties being driven by its fiber architecture. Electrospun scaffolds with templated architectures were characterized with regard to fiber alignment and mechanical properties. Fast Fourier transform analysis revealed a high degree of fiber alignment along the conducting traces of the templates. Mechanical testing showed that scaffolds demonstrated tunable mechanical properties as a function of templated architecture. Fibroblast seeded scaffolds were subjected to a peak strain of 3% or 10% at 0.5 Hz for 1 hour. Exposing seeded scaffolds to the low strain magnitude (3%) significantly increased collagen I gene expression compared to the high strain magnitude (10%) in a scaffold architecture dependent manner. These experiments indicate that scaffolds with templated architectures can be produced and modulation of gene expression is possible with templated architectures. This technology holds promise for the long term goal of creating tissue engineered replacements with the biomechanical and biochemical make-up of native tissues.

Keywords

electrospinning; tissue engineering; anisotropic scaffold; collagen I; cyclic strain

Introduction

The use of electrospinning to produce small diameter fibers has been conducted since the early 20th century[1, 2]. More recently, electrospinning has garnered widespread attention in the tissue engineering field[3-5] for the production of scaffolds capable of recapitulating the extracellular matrix (ECM) of native tissue (biomimetic scaffolds). Such applications necessitate more sophisticated electrospun scaffolds to mimic the complicated architecture and anisotropy of native ECM. Unfortunately, traditional electrospinning templates result in unorganized or uniaxially aligned fibers.

Numerous collector types have been used over the years to control the electrospinning jet[6-9]. In general, two collector methodologies have been employed to align the fibers: dynamic

Correspondence to: A. Karchin.

mechanical devices, or electrical manipulation of the collection surface. Electrical manipulation is typically achieved through a collection surface made up of conductive wires or strips separated by an insulating gap. This collection technique has multiple advantages compared to dynamic collection (e.g. rotating mandrel); electrical manipulation can be achieved with a simpler set-up, and avoids the potential deleterious effects that a rotating collector can have on the mechanical properties of electrospun fibers[10]. What is lacking, however, is an electrospinning template which allows for collection of highly aligned fibers along multiple, non-orthogonal axes. Such a template is important in the design of tissue engineering scaffolds for replacement of complex tissue structures such as tendons and ligaments.

A tissue engineered replacement for soft tissue structures such as ligaments and tendons should include both topographical cues to orient cells relative to the applied strain direction, and adequate mechanical stimulation to induce ECM deposition. Fibroblasts cultured on smooth surfaces subject to uniaxial strain tend to orient perpendicular to the strain direction[11-13], likely to avoid large axial strains[14]. However, fibroblasts growing on native ligaments are aligned along the predominant stretch direction guided by the parallel arrangement of fibrillar collagen. Since contact guidance has been shown to prevent reorientation of cultured fibroblasts in response to cyclic uniaxial strain[15], it has been described as the dominant mechanism[15] when it comes to directing cellular response to strain. Contact guidance cues most readily act to reorient the cytoskeleton which precedes cellular alignment in response to strain[12] and have been shown to lead to production of aligned collagenous matrix[16]. Providing an organized template on which to culture cells is relevant in the design of tissue engineered scaffolds since oriented fibroblasts will deposit greater amounts[17] of correctly oriented[16] ECM. A fibrous scaffold can therefore be thought of as a template for the engineered graft providing the organizational framework of the eventual replacement ECM.

The current study sought to mediate cell response through scaffold mechanical behavior. It was hypothesized that mechanical stimulation of cell-seeded electrospun scaffolds with templated architecture will result in tunable collagen expression. The first objective was to fabricate scaffolds whose bulk mechanical properties were driven by fiber architecture, herein referred to as templated architecture. Towards this goal, a novel technique to fabricate patterned electrospinning templates is described, and electrospun scaffolds using these templates were characterized with respect to fiber alignment and key mechanical properties. The second objective was to determine if mechanical differences in templated architecture translated to differences in gene expression, specifically collagen I. This was accomplished by quantifying gene expression from cell-seeded scaffolds with templated architecture subject to cyclic mechanical stimulation *in vitro*. To the authors' knowledge, an electrospun template which can achieve fiber orientation along multiple non-orthogonal axes in a single scaffold layer is a novelty.

Materials and Methods

2.1 Template Fabrication

Electrospinning templates were made from phenolic boards with inlaid copper traces using standard printed circuit board manufacturing technique. All supplies were purchased from MG Chemicals (Surrey, British Columbia). Images of the desired template design were created with freely available computer aided design (CAD) software (ExpressPCB, Santa Barbara, CA) and templates fabricated according manufacturer's instructions.

Different template designs were used to achieve scaffolds with templated architecture: parallel and diamond (Figure 1). Parallel templates were made up of traces parallel to the

longitudinal axis of the rectangular template. Diamond templates were made up of traces oriented at 45° and -45° to the longitudinal axis. All templates contained traces that were 0.15 mm wide and spaced 2.5 mm apart. As a control, unaligned scaffolds were collected on a strip of adhesive backed copper mounted on a glass slide. All samples were collected in a single electrospinning run with scaffolds from each architecture and trace spacing collected in random order.

2.2 Electrospinning

All samples were prepared in a custom apparatus developed in our lab, described previously[18]. Commercially available polyurethane (Estane 58315, BF Goodrich, Cleveland, OH) was used in this study. Raw polymer was melted in a metal sleeve terminating in a 2 mm diameter nozzle in an oven at 150°C under vacuum to remove bubbles formed during melting. The sleeve was then transferred to the melt chamber of the electrospinning apparatus where the temperature was raised and held to 250°C for electrospinning. The distance between positive and ground electrodes was set to 16 cm with a potential of 25 kV between them. Templates were mounted on a 3-axis stage 10 cm from the ground. To ensure complete coverage of the template, the stage was moved in a raster pattern underneath the electrospinning head with 4 mm displacement in the longitudinal direction and 2 mm displacement in the orthogonal direction. An auxiliary power supply was clipped to the template with an alligator clip which supplied a potential of 20 kV.

2.3 Fiber alignment

Fiber alignment was evaluated using techniques based on those developed by Ayres *et al*[19]. Images of scaffolds were visualized with an optical microscope (Eclipse 80i, Nikon, Melville, NY) and digitized with a 12.6 Megapixel digital camera (DXM-1200C, Nikon, Melville, NY). Brightfield images were captured with a 2× objective and stored as .TIF files.

Scaffold images were imported into Adobe Photoshop Elements (Adobe Systems Incorporated, San Jose, CA) to parse into location-specific crops. To simplify the analysis, diamond images were rotated 45° counterclockwise so that all traces were either vertically or horizontally oriented. Round crops were cut from scaffold images in two key locations (Figure 2): 1) over traces and 2) the center region that is midway between adjacent traces. Two crops were taken for each location within a given scaffold image with three scaffolds analyzed for each architecture. Masked images were imported into Image J (v1.42q, National Institute of Mental Health, Bethesda, MD) for FFT analysis. The oval profile plug-in (authored by William O'Connell) was used to plot summed pixel intensities at 1° increments (0°–360°) versus their corresponding radial position around the unit circle.

Summed pixel intensity data and their corresponding radial position were imported into Excel (Microsoft Corporation, Redmond, WA) for analysis of fiber alignment. An alignment ratio was determined by integrating and dividing data clustered around 90° (60°–120°) to 180° (150°–210°) using a custom algorithm in Matlab (The Mathworks, Inc, Natick, MA). Each image was rotated 90° and re-analyzed to normalize vertically and horizontally oriented fibers. Native and rotated alignment ratios were averaged for a final alignment ratio mean.

Using statistical software (SPSS, Chicago, IL), a one-way independent ANOVA and post hoc tests (Tukey and Games-Howell) were performed on the alignment ratio to determine statistical significance ($p < 0.05$) between fibers over traces vs. between traces, over traces vs. unaligned scaffold, and between traces vs. unaligned scaffold.

2.4 Tensile testing

Testing was performed following ASTM standard D5035 (Standard Test Method for Breaking Force and Elongation of Textile Fabrics - Strip Method). Rectangular samples (5×26 mm) were subject to a tensile test under displacement control at 50 mm/min until failure in an Instron testing machine (5543, Instron, Norwood, MA). Test strips were cut at either a parallel (0°) or orthogonal (90°) orientation to the longitudinal axis of the rectangular templates.

For strain calculations, the initial gauge length was taken as the grip-to-grip distance of 15 mm. For stress calculations, the bulk thickness of each sample was measured in three locations with a digital micrometer while the sample was at zero displacement in the Instron. To compute the cross sectional area, bulk width and thickness measurements were multiplied by fiber area fraction, determined as described below. The tangent modulus was computed from the slope of the linear region of the stress–strain curves. The linear region was defined as the segment over which the best fit linear regression had an R^2 greater than 0.999.

Using statistical software (SPSS, Chicago, IL), a one-way independent ANOVA and post hoc tests (Tukey and Games-Howell) were performed on the inflection strain, ultimate tensile stress (UTS) and ultimate strain to determine statistical significance ($p < 0.05$) between 0° and 90° oriented samples, and between architectures. The inflection strain was taken as the upper boundary of the toe region signifying the start of the linear elastic region. Five samples of each architecture were tested.

2.5 Local Strain

Since local strain of fibrous materials is different than applied bulk strain, image analysis was used to assess local strain in the scaffold gauge length. The markers were oriented along the longitudinal direction and placed in different locations for each scaffold architecture:

- parallel scaffolds - along a single fiber bundle
- diamond scaffolds - at the diamond apices
- unaligned scaffolds - along a single line parallel to the longitudinal axis

Scaffolds were then subject to three levels of fixed bulk strain: 0% (i.e. neutral position), 3%, and 10%. The two levels of strain were chosen to match the stimulation protocol discussed below. Images were acquired with a digital camera (SD940, Canon USA, Lake Success, NY) mounted on a tripod at each strain level. Images were acquired immediately after strain was applied to minimize stress relaxation. Strain was calculated by measuring the edge-to-edge distance between dots with the straight line tool in Image J software. Data were acquired from three scaffolds of each architecture.

2.6 Fiber Morphology

Fiber area fraction was determined by taking measurements of individual fibers based on un-biased stereological techniques[20]. To accomplish this measurement, three scaffolds within each architecture were first embedded in optimal cutting temperature medium and flash frozen in isopentane pre-cooled on dry ice. Random equidistant 12 μm sections were cut from the frozen blocks with a cryostat (Cryotome E, Shandon, Inc, Pittsburgh, PA). Sections were digitized with an optical microscope at 20× by taking a random 0.35 mm^2 image. Images were imported into Image J and converted to binary threshold. Calculation of fiber area fraction was accomplished with the area fraction measurement tool. The fiber diameter was taken as the minimum Feret's diameter. The average fiber diameter and its distribution were determined from 200 to 225 measurements taken from all sections.

2.7 Cell culture

It was desirable to establish a fibroblast cell line from a collagen–rich load bearing soft-tissue structure. Hence, anterior cruciate ligaments were aseptically harvested from a single freshly sacrificed adolescent Yorkshire pig. In a biosafety cabinet, ligaments were minced to facilitate cell outgrowth according to Protocol 11.4 of Freshney[21]. Prior to mincing, all fascia and extra tissue was vigorously scraped away from the ligaments with a scalpel blade. The remaining tissue was then put through a series of ten swirling washes of 5% 100× antibiotic/antimicrobial (15240-062, Invitrogen, Carlsbad, CA) in phosphate buffered saline (PBS) in individual sterile Petri dishes. The tissue was then moved to a clean Petri dish and minced into ~1 mm^3 cubes with two crossing scalpel blades. Cubed tissue was sparsely placed in multiple 60 mm Petri dishes with a minimal amount of culture medium so that the tissue stuck to the bottom of the dish. Dishes were placed in an incubator with 37°C humidified atmosphere of 5% CO_2. Once the explants stuck to the bottom of the dish, typically 1–2 days, more culture medium was added. Fibroblast migration typically took 5–7 days, during which medium was changed every three days. Once cells approached 70% confluence tissue was removed. Cells were trypsinized (T4049, Sigma-Aldrich, St. Louis, MO) and re-plated once the colony approached 70% confluence; cells from passage 6 were used for seeding.

All cell culture medium ingredients were obtained from Sigma-Aldrich (St. Louis, MO) unless otherwise noted. The cell culture medium consisted of Dulbecco's Modified Eagle's Medium (DMEM) (D5796) supplemented with 10% fetal bovine serum (FBS) (SH3008802, Fisher Scientific, Pittsburg, PA), 1% L-glutamine (G7513), 1% 100× antibiotic/antimicrobial (15240-062, Invitrogen, Carlsbad, CA), and Hepes buffer (H0887).

Prior to cell seeding, electrospun scaffolds were washed and sterilized in a similar manner described previously[22]. Scaffolds were coated with 10 μg/ml fibronectin before seeing with fibroblasts (1.5×10^6 cells/ml). To maximize seeding efficiency, scaffolds were placed on a Parafilm sheet and exposed to the concentrated cell slurry for 2 hours in an incubator. After this time, fresh medium was added until scaffolds were submersed.

2.8 Scanning electron microscopy (SEM)

To determine the morphology of cells growing on unstrained scaffolds, seeded scaffolds were cultured for two weeks prior to fixation with Karnovsky's fixative for electron microscopy (15720, Electron Microscopy Sciences, Hatfield, PA). Cellular morphology was visualized from SEM (Sirion, FEI Company, Eindhoven, The Netherlands) micrographs. Prior to visualization, samples were sputter-coated for 30 seconds forming an approximately 10 nm thick gold layer in order to prevent charging. The micrographs were taken using an accelerating voltage 5 kV for the electrospun samples.

2.9 Bioreactor

Seeded scaffolds were subject to mechanical stimulated in a custom designed bioreactor integrated into a load application system (LAS)[23]. Three days before seeded scaffolds were subject to mechanical stimulation, they were loaded into the sterile bioreactor. Scaffolds were first affixed to a clamp assembly in a bath of sterile PBS. Once all the scaffolds were clamped, the clamp assembly was removed from the PBS and placed in a bioreactor chamber pre-filled with the aforementioned culture medium. The bioreactor was then placed in an incubator until mechanical stimulation. Two days prior to mechanical stimulation, the cell culture medium was changed to a synchronization medium. Seeded scaffolds were maintained in the synchronization medium for the duration of the stimulation time. All synchronization medium ingredients were obtained from Sigma-Aldrich (St. Louis, MO) unless otherwise noted. The synchronization medium consisted of DMEM supplemented

with 1% penicillin-streptomycin (4333), 1% non-essential amino acids (M7145), 1% universal culture supplement (354352, BD Biosciences, San Jose, CA), 0.1 μM dexamethasone (D4902), 40 μg/mL L-proline (P5607), 50 μg/mL ascorbate 2-phosphate (A8960), and 100 μg/mL sodium pyruvate (BP356-100, Fisher Scientific, Pittsburg, PA).

2.10 Mechanical Stimulation Protocol

For the mechanical stimulation procedure, the bioreactor was transferred from the incubator to the LAS and carefully placed in a recessed port on the top of the air plenum. Seeded scaffolds from each architecture were separated into three groups:

- high strain level: 10% nominal strain at 0.5 Hz for 1 hour
- low strain level: 3% nominal strain at 0.5 Hz for 1 hour
- sham control: in LAS for 1 hour with no strain applied

The nominal strain was the applied strain at the grips based on the gauge length.

2.11 RNA isolation

Total RNA was isolated from cell-seeded scaffolds by cutting out the gauge length immediately placing the sample in an RNase-free mortar and pestle (K749520-0090, Fisher Scientific, Pittsburg, PA) in the presence to Tri Reagent® (T9424, Sigma-Aldrich, St. Louis, MO). RNA isolation was performed according to the manufacturer's instructions. Samples were re-suspended in TE buffer (10 mM Tris-HCL, 1mM EDTA) to 45 μl and concentration determined with a spectrophotometer (170-2525, Bio-Rad Laboratories, Inc., Hercules, CA).

2.12 Gene Expression

Expression of collagen I and the housekeeping gene, Glyceraldehyde 3-phosphate dehydrogenase (GAPDH), were determined by real-time polymerase chain reaction (PCR) using an Applied Biosystems 7900HT SDS instrument. Porcine specific primers were obtained from Applied Biosystems (Foster City, CA) for collagen I (ss03373341 g1) and GAPDH (ss03373286 u1). Each reaction was performed in triplicate. Mean and standard deviation values were used in the comparative threshold method (ΔΔCt) according to Perkin-Elmer ABI Prism 7700 User Bulletin #2. The ΔΔCt parameter was computed for the strained scaffold relative to no strain control, normalized to GAPDH expression, for each architecture.

Scaffolds from the three mechanical stimulation groups contained four scaffolds of each architecture. Using statistical software (SPSS, Chicago, IL), a one-way independent ANOVA and post hoc tests (Tukey and Games-Howell) was performed on the means to determine statistical significance ($p < 0.05$) between the two mechanical stimulation groups with respect to scaffold architecture.

Results

Scaffolds electrospun onto the parallel and diamond templates closely matched the macroscopic template architecture (Figure 2) with fibers aligned along the trace regardless of template architecture. In addition to trace alignment, fibers preferentially aggregated along traces with minimal fibers appearing between traces. Electrospun scaffolds did not adhere to the templates, and could be easily removed from the template with no damage or distortion to the scaffold. Irrespective of architecture, scaffolds contained fibers with a mean fiber diameter of 36.9 ± 9.0 μm and an overall average thickness of 318.6 ± 50.2 μm. The mean fiber area fraction was 7%, 8.6% and 7.6% for diamond, parallel, and unaligned scaffolds, respectively.

A pilot study was performed to determine the effect that trace width and trace spacing (i.e. distance between traces) had on fiber alignment (data not shown). Trace width in the ExpressPCB CAD software could be adjusted from 0.15–6.35 mm. Templates were fabricated with traces that were 0.15, 0.18, 0.20, 0.25, and 0.30 mm wide. Fibers were electrospun onto the templates and examined microscopically to get a qualitative assessment of the relationship between trace width and fiber alignment. It was observed that the narrower the traces resulted in greater fiber alignment. These results are similar to previously published work[9]. Therefore all subsequent templates were made with a 0.15 mm trace width.

3.1 Fiber Alignment

Example data from each of the three key locations are shown in Figure 3. Alignment along the traces is recognized by the prominent peaks (Figure 3A and C). The height and narrow width of the peaks is indicative of a high degree of fiber alignment. The center regions of parallel scaffolds (Figure 3B) exhibited fiber alignment orthogonal to the trace orientation. No distinct peaks are noted in the diamond center regions (Figure 3D).

The alignment ratio mean at each of the three key locations for each scaffold architecture is presented in Table 1. Fibers that have no preferential orientation would have normalized area close to 1, while values greater and less than 1 indicate alignment in a parallel and orthogonal direction, respectively. Fibers which lay over traces in both architectures have significantly greater areas than both the unaligned scaffolds (parallel: $p = 0.008$; diamond: $p = 0.019$) and the respective center regions (parallel: $p = 0.005$; diamond: $p = 0.012$). The mean center region area of 0.54 for the parallel scaffolds indicates that fibers in this region are fairly well aligned in the orthogonal direction between traces. Of note are fibers which lay at the intersection of two traces which can be seen to be aligned along the orthogonal traces (Figure 2B). Two modes of alignment are observed in this region. First, fibers can be seen to be aligned along the orthogonal traces. Second, some fibers can be seen to change direction from one trace to another. This second mode somewhat confounded the analysis for the diamond trace regions contributing to the difference in sharpness between parallel (Figure 3A) and diamond peaks (Figure 3C).

3.2 Mechanical properties

Scaffolds from all architectures had a tangent modulus of approximately 1 MPa. Other mechanical properties for scaffolds of both orientations for all architectures are presented in Table 2. Parallel scaffolds exhibited evidence of anisotropy. The UTS of samples cut at 0° was significantly higher than those cut at 90° ($p = 0.032$). However, statistical analysis failed to detect evidence of anisotropy in the ultimate strain for parallel scaffolds. Diamond and unaligned samples exhibited no anisotropy as evidenced by the lack of statistical significance in UTS and ultimate strain between sample orientations.

Scaffold architecture had a significant effect on mechanical properties. Unaligned scaffolds tested at 0° had significantly lower UTS than the parallel ($p = 0.004$) and diamond scaffolds ($p = 0.048$) with the same orientation. Diamond scaffolds had significantly greater inflection strain than the parallel ($p = 0.004$) and unaligned scaffolds ($p = 0.005$). Taken together, these data indicate that through the design of the electrospinning template, directed anisotropy and tunable mechanical properties can be imparted to electrospun scaffolds using the current template manufacturing technique.

Local strains were consistently smaller than bulk strain (Table 3). Image analysis of local strain revealed that the low and high nominal strain level resulted in mean strains of 0.9% and 2.1%, respectively, along the fiber bundles in the parallel scaffolds. The unaligned

scaffolds experienced 0.7% and 2.6% mean strain, respectively, for the low and high strain level in the unaligned scaffolds, while the diamond scaffolds experienced virtually no strain along the fiber bundles. The negative strain values measured for the diamond scaffold indicate that the nodes are moving closer together when this architecture is stretched.

3.3 Cell culture

Cells infiltrated throughout the scaffolds with viable cells seen both on the outside and within fiber bundles. SEM evaluation revealed that cell penetration within scaffolds and fiber bundles did not vary as a function of architecture. There was a higher density of cells in areas of aligned fibers simply due to there being a higher density of fibers in these areas.

Fibroblasts cultured on parallel and diamond scaffolds elongated along individual fibers or bundles of fibers when fibers were close packed. Individual cells mostly elongated along individual fibers rather than stretching between adjacent fibers; however, when cells encountered a fiber point bond (“spot weld” between two crossing non-parallel fibers) they assumed a pyramidal morphology. This morphology was observed in three locations: 1) when fibers crossed in the region between conductive traces in parallel templates, 2) at the intersection of orthogonal traces in diamond templates, and 3) on unaligned scaffolds.

3.4 Gene Expression

Changes in collagen I expression were found to be both strain and architecture dependent. Cells growing on parallel scaffolds subject to the low strain level expressed significantly ($p = 0.042$) more collagen I than those growing on diamond scaffolds (Figure 5). The low strain level also induced significantly greater collagen I expression over the high strain level for parallel ($p = 0.033$) and unaligned ($p = 0.029$) scaffolds.

Discussion

The presented electrospinning template technique utilizes the precision of CAD design to produce a template with distinct organization resulting in an electrospun scaffold made up of aligned fibers in a controlled architecture. For tissue engineering applications, the ability to align scaffolds along multiple axes is critical to recapitulate complex tissues. A significant advantage of the current template technology over others, such as a rotating mandrel, is the ability to make scaffolds with complex fiber alignment in a single electrospun layer.

A trace spacing below 2.0 mm resulted in greater fiber aggregation between the traces instead of distinct bundles of aligned fibers along the traces. Trace spacing greater than 3.0 mm resulted in few fibers between the traces. This presented two problems for the current study. First, the intended gauge width for seeded samples was 5.0 mm so a 3.0 mm trace distance did not result in enough fiber bundles in the gauge area. Second, scaffolds that were predominately made up of fiber bundles were assumed to be too “flimsy” for future long term cell mechanical stimulation studies. Therefore, trace spacing of 2.5 mm were evaluated for this study. The conclusion of this pilot study was that when the charged template surface is composed of wide or very close together traces, it acts more like a simple flat plate collector which results in no preferential alignment of collected electrospun fibers.

Electrospun fibers that are ejected from the nozzle are highly charged, taking on the polarity of the electrode placed in the melt. Due to the bending instability of the fiber path, its motion is chaotic. However, when a polar-opposite charged template is placed in this path, fiber-template electrostatic interaction dominates. The net effect of this attraction is alignment of fibers along the charged traces. The ability of a trace to align fibers parallel to its longitudinal axis depends on the width of the trace. When a conducting trace is wide compared to a fiber's diameter, the large surface decreases the probability that the fiber will

lie parallel to the longitudinal axis. The preference of fibers to align normal to traces in the parallel architectures is similar to previously published results. Li *et al*[24] demonstrated alignment between adjacent conductive substrates separated by a non-conducting void gap. Once a fiber is deposited across the gap, repulsive Coulombic forces between fibers serve to push fibers into a parallel arrangement while the charge of the trace pulls fibers across the gap. In the current study complex fiber architecture was achieved in a single scaffold layer. To the authors' knowledge, this is a novelty in the electrospinning literature.

Fiber alignment analysis and tensile testing demonstrated the presence of anisotropy and tunable mechanical properties. The preferential alignment of fibers along parallel template traces (i.e. along the 0° testing orientation) yielded scaffolds that were approximately 30–100% stronger than the orthogonal direction and other architectures. Ligaments and tendons are known to exhibit anisotropic behavior due to the primarily uni-axial alignment of the collagen fiber bundles which makes up these tissues' ECMs. Due to their architecture, tendons and ligaments are adept at transmitting primarily tensile forces oriented along their longitudinal axes. A study to characterize the anisotropic material properties of the human medial collateral ligament (MCL) found an approximately 2000% increase in UTS of samples cut from the longitudinal direction compared to those cut from the traverse direction[25]. In contrast, the glenohumeral joint which is considered to function in a multi-axial manner was found to have an UTS 150% higher in samples cut from the longitudinal direction compared to those cut from the transverse direction[26]. Hence while the scaffolds tested in the current study do not explicitly match the mechanical properties of many native tissues, this method of aligning electrospun fibers is effective at controlling scaffold anisotropic behavior. The demonstration that scaffolds electrospun with the novel template exhibit templated architecture satisfies the primary objective of this study.

Preferential alignment along the crisscrossing traces of the diamond templates yielded scaffolds that lacked anisotropy, however, had significantly greater inflection strain (i.e. toe region) than the other architectures. The toe region, characteristic of stress-strain curves of soft biological tissue, is the low stiffness portion of the curve and attributed to the uncrimping of collagen fibers. Once uncrimped, elongated collagen fibers resist tensile loading exhibiting linear behavior on the curve. Human knee ligaments, anterior cruciate ligament (ACL) and medial collateral ligament (MCL), have toe regions spanning 2.0–4.8% in length[27]. Functional tissue engineered solutions should mimic the mechanical behavior of the tissues they are intended to replace. Again, while the scaffold architectures made in the current study do not explicitly match those of the ACL or MCL, what is clear is that architecture can be adjusted to tune mechanical properties. At low strains, fibers in the diamond architecture undergo a re-organization aligning along the principal strain direction. During re-organization the fibers gradually align to resist tension. In contrast, fibers in the parallel scaffolds are readily available to resist tension immediately given their predominant initial orientation.

For all scaffolds preferential alignment and aggregation along conducting traces with minimal fibers appearing between traces was observed. A goal of this work was to demonstrate that alterations in mechanical cues, driven by scaffold architecture, lead to alterations in collagen I gene expression. Hence, minimizing fibers in the unaligned areas of the parallel and diamond scaffolds as fibers in these regions would not reliably deliver the mechanical cues like fibers in the aligned regions was preferable. This was an advantage of the current electrospinning alignment technique since the resultant scaffold was predominantly composed of highly aligned fibers. There was a higher density of cells in areas of aligned fibers simply due to there being a higher density of fibers in these areas. Based on the similar fiber area fractions, there were not large differences between surface areas into which cells could grow between scaffold architectures. The intention was to have

the areas of unaligned fibers sparsely populated with cells since these areas will not impart the primary mechanical cues accordant with the aligned fiber fibers.

The low strain level brought out the most substantial differences in collagen I expression between architectures with cells growing on parallel scaffolds expressing significantly more collagen I than cells growing on diamond scaffolds. Conversely, the high strain level did not result in appreciable difference in collagen I expression between architectures. While these data support a strain magnitude threshold below which collagen I is stimulated and above which expression it is inhibited, it was an unexpected result. All the measured local strain magnitudes are within 0–4.4% experienced by the ACL during typical rehabilitation activities (e.g. squatting, stair climbing, and stationary bicycling)[28], but below the higher levels typically applied in *in vitro* studies which have demonstrated that collagen I expression increases in response to mechanical stimulation[14, 29, 30]. It was therefore expected the collagen I expression would increase in a strain dependent manner up to a threshold.

For the strain magnitudes tests, collagen I expression was greater at local strains in the neighborhood of 0.7–0.9%, whereas local strains approximately above 2.1% and below 0% did not increase collagen production over control scaffolds. The strain values observed along the trace of the diamond scaffolds indicate a more complicated loading pattern. The negative strain values indicate that the nodes are moving closer together as the diamond is stretched. This motion would cause the segment between the nodes to experience a combination of bending, shear, and tension between the fibers in the segment. The presence of an expression threshold relative to strain level matches previously published results[31]. The authors in previous studies observed an increase in collagen I expression in response to tensile strain to 20% then a decrease at 40%. However, it is not feasible to quantitatively compare the effects of strain level due to experimental differences such as cell type, scaffold material architecture, medium recipe, and mechanical stimulation regime.

While future study is warranted to more accurately model the deformation behavior scaffolds with templated architecture has on a small scale (e.g. with a finite element model), the observation that collagen I expression can be moderated through scaffold architecture satisfies the secondary objective of this study. It was hypothesized that mechanical stimulation of cell-seeded electrospun scaffolds with templated architecture will result in tunable collagen expression. Image analysis of the parallel and diamond scaffolds validate the different magnitudes of local strain experienced by architecture. No difference in collagen I expression was noted in control scaffolds between architectures (data not shown). Hence, it was the mechanical stimulation magnitude, mediated by fiber architecture, which resulted in gene expression. Taken together, these data support the conclusion that stretching scaffolds with templated architecture yields differing mechanical cues capable of moderating collagen I expression.

Limitations of the current study must be noted. One limitation was the limited number of number of mechanical stimulation regimes employed. The scaffolds were exposed to a single dose of cyclic strain at a single frequency. Fibroblasts have been shown to mediate collagen I expression levels in a frequency-dependent manner[29], and in response to stimulation duration[32] and duty cycle[33]. While a single, short dose of cyclic strain at 0.5 Hz has been shown to significantly affect collagen I expression[29, 30], future studies should include a more thorough exploration of stimulation regime parameters to overcome this limitation. Another limitation is that the scaffolds used in this study had fibers that are larger than collagen fibers in native tissue. Scaffolds from all architectures contained fibers that had a mean diameter of 36.9 μm, while the ACL contains collagen fibers in the 1–20 μm range[34]. Collagen I expression has been shown to be sensitive to scaffold fiber diameter[35];

therefore future studies should more tightly regulate the fiber diameter in electrospun scaffolds to eliminate this limitation. This can be achieved by altering electrospinning processing parameter such as electric field strength, polymeric viscosity, and flow rate[36]. While these limitations should be overcome in future studies, they do not detract from the stated goals of the current study since a clear dependence of collagen I expression on scaffold architecture was observed.

Further, quantification of local strain directly experienced by embedded cells was not determined. Screen *et al*[37] stained tendon fibroblasts with a fluorescent dye Acridine Orange, a nuclear stain, to quantify local strains within collagen fascicles subject to bulk strain. The authors found that local strains within the fascicle was always smaller than applied strains, and even with bulk strains up to 8%, local strains never exceeded 15% of the bulk strains. Local strains measured in the parallel and unaligned scaffolds ranged from 21–29% of the applied strain. Hence, the assumption that local scaffold strains measured via image analysis translate to actual cell strain remains to be validated.

Conclusion

The primary objective of this study was to develop a novel electrospinning template which allowed for collection of scaffolds with complex templated architecture. Using this method, scaffold anisotropy and mechanical properties could be tuned through the design of templated architecture. The modulation of collagen expression via mechanical stimulation of seeded scaffolds with templated architecture was presented. This result suggests that collagen expression tuning can be driven by scaffold architecture. These studies provide the groundwork for future work in which a heterogeneous biochemical make-up of a tissue engineered graft can be “designed” on the front end through a specific arrangement of scaffold architecture.

Acknowledgments

We are grateful to Dr. David G. Simpson for his generous assistance with the 2D FFT technique, and to Dr. Ed J. Kelly of the UW Center for DNA sequencing and Gene Analysis for performing the PCR work. In addition, the authors are grateful to Dr. Paul D. Dalton for the invaluable discussions regarding electrospinning. The authors would also like to acknowledge the funding sources which enabled this work. These included University of Washington Engineered Biomaterials (UWEB) under the direction of Dr. Buddy D. Ratner, and NIH RO1 HD038554. In addition, Dr. Karchin was funded through the Engineered Biomaterials Training Program (EBTP).

References

1. Cooley, J. 1902: US.
2. Morton, W. 1902: US.
3. Kumbar SG, James R, Nukavarapu SP, Laurencin CT. Electrospun nanofiber scaffolds: engineering soft tissues. Biomed Mater. 2008; 3(3):034002. [PubMed: 18689924]
4. Boland ED, Matthews JA, Pawlowski KJ, Simpson DG, Wnek GE, Bowlin GL. Electrospinning collagen and elastin: preliminary vascular tissue engineering. Front Biosci. 2004; 9:1422–32. [PubMed: 14977557]
5. Nair LS, Bhattacharyya S, Laurencin CT. Development of novel tissue engineering scaffolds via electrospinning. Expert Opin Biol Ther. 2004; 4(5):659–68. [PubMed: 15155157]
6. Li D, Ouyang G, McCann JT, Xia Y. Collecting electrospun nanofibers with patterned electrodes. Nano Lett. 2005; 5(5):913–916. [PubMed: 15884893]
7. Matthews JA, Wnek GE, Simpson DG, Bowlin GL. Electrospinning of collagen nanofibers. Biomacromolecules. 2002; 3(2):232–8. [PubMed: 11888306]
8. Teo WE, Ramakrishna S. A review on electrospinning design and nanofibre assemblies. Nanotechnology. 2006; 17:R89–R106. [PubMed: 19661572]

9. Zhang D, Chang J. Patterning of Electrospun Fibers Using Electroconductive Templates. Adv Mat. 2007; 19:3664–3667.
10. Zussman E, Rittel D, Yarin AL. Failure modes of electrospun nanofibers. Applied Physics Letters. 2003; 82(22):3958–3960.
11. Park SA, Kim IA, Lee YJ, Shin JW, Kim CR, Kim JK, Yang YI. Biological responses of ligament fibroblasts and gene expression profiling on micropatterned silicone substrates subjected to mechanical stimuli. J Biosci Bioeng. 2006; 102(5):402–12. [PubMed: 17189167]
12. Neidlinger-Wilke C, Grood E, Claes L, Brand R. Fibroblast orientation to stretch begins within three hours. J Orthop Res. 2002; 20(5):953–6. [PubMed: 12382959]
13. Loesberg WA, Walboomers XF, van Loon JJ, Jansen JA. The effect of combined cyclic mechanical stretching and microgrooved surface topography on the behavior of fibroblasts. J Biomed Mater Res A. 2005; 75(3):723–32. [PubMed: 16110493]
14. Kim SG, Akaike T, Sasagaw T, Atomi Y, Kurosawa H. Gene expression of type I and type III collagen by mechanical stretch in anterior cruciate ligament cells. Cell Struct Funct. 2002; 27(3): 139–44. [PubMed: 12207044]
15. Wang JH, Yang G, Li Z. Controlling cell responses to cyclic mechanical stretching. Ann Biomed Eng. 2005; 33(3):337–42. [PubMed: 15868724]
16. Wang JH, Jia F, Gilbert TW, Woo SL. Cell orientation determines the alignment of cell-produced collagenous matrix. J Biomech. 2003; 36(1):97–102. [PubMed: 12485643]
17. Lee CH, Shin HJ, Cho IH, Kang YM, Kim IA, Park KD, Shin JW. Nanofiber alignment and direction of mechanical strain affect the ECM production of human ACL fibroblast. Biomaterials. 2005; 26(11):1261–70. [PubMed: 15475056]
18. Mitchell SB, Sanders JE. A unique device for controlled electrospinning. J Biomed Mater Res A. 2006; 78(1):110–120. [PubMed: 16604530]
19. Ayres CE, Jha BS, Meredith H, Bowman JR, Bowlin GL, Henderson SC, Simpson DG. Measuring fiber alignment in electrospun scaffolds: a user's guide to the 2D fast Fourier transform approach. J Biomater Sci Polym Ed. 2008; 19(5):603–621. [PubMed: 18419940]
20. Gundersen HJ, Osterby R. Optimizing sampling efficiency of stereological studies in biology: or ‘do more less well!’. J Microsc. 1981; 121(Pt 1):65–73. [PubMed: 7014910]
21. Freshney, RI. Culture of animal cells : a manual of basic technique and specialized applications. 6th. Hoboken, N.J.: John Wiley & Sons; 2010.
22. Sanders JE, Malcolm SG, Bale SD, Wang YN, Lamont S. Prevascularization of a biomaterial using a chorioallontoic membrane. Microvasc Res. 2002; 64(1):174–8. [PubMed: 12074644]
23. Mitchell SB, Sanders JE, Garbini JL, Schuessler PK. A device to apply user-specified strains to biomaterials in culture. IEEE Trans Biomed Eng. 2001; 48(2):268–273. [PubMed: 11296883]
24. Li D, Wang Y, Xia Y. Electrospinning Nanofibers as Uniaxially Aligned Arrays and Layer-by-Layer Stacked Films. Advanced Materials. 2004; 16(4):361–366.
25. Quapp KM, Weiss JA. Material characterization of human medial collateral ligament. J Biomech Eng. 1998; 120(6):757–63. [PubMed: 10412460]
26. Moore SM, McMahon PJ, Azemi E, Debski RE. Bi-directional mechanical properties of the posterior region of the glenohumeral capsule. J Biomech. 2005; 38(6):1365–9. [PubMed: 15863121]
27. Freeman JW, Woods MD, Laurencin CT. Tissue engineering of the anterior cruciate ligament using a braid-twist scaffold design. J Biomech. 2007; 40(9):2029–36. [PubMed: 17097666]
28. Fleming BC, Beynnon BD, Renstrom PA, Johnson RJ, Nichols CE, Peura GD, Uh BS. The strain behavior of the anterior cruciate ligament during stair climbing: an in vivo study. Arthroscopy. 1999; 15(2):185–91. [PubMed: 10210077]
29. Gilbert TW, Stewart-Akers AM, Sydeski J, Nguyen TD, Badylak SF, Woo SL. Gene expression by fibroblasts seeded on small intestinal submucosa and subjected to cyclic stretching. Tissue Eng. 2007; 13(6):1313–23. [PubMed: 17518717]
30. Yang G, Crawford RC, Wang JH. Proliferation and collagen production of human patellar tendon fibroblasts in response to cyclic uniaxial stretching in serum-free conditions. J Biomech. 2004; 37(10):1543–50. [PubMed: 15336929]

31. Powell HM, McFarland KL, Butler DL, Supp DM, Boyce ST. Uniaxial strain regulates morphogenesis, gene expression, and tissue strength in engineered skin. Tissue Eng Part A. 2010; 16(3):1083–92. [PubMed: 19845460]

32. Hsieh AH, Tsai CM, Ma QJ, Lin T, Banes AJ, Villarreal FJ, Akeson WH, Sung KL. Time-dependent increases in type-III collagen gene expression in medical collateral ligament fibroblasts under cyclic strains. J Orthop Res. 2000; 18(2):220–7. [PubMed: 10815822]

33. Juncosa-Melvin N, Matlin KS, Holdcraft RW, Nirmalanandhan VS, Butler DL. Mechanical stimulation increases collagen type I and collagen type III gene expression of stem cell-collagen sponge constructs for patellar tendon repair. Tissue Eng. 2007; 13(6):1219–26. [PubMed: 17518715]

34. Strocchi R, de Pasquale V, Gubellini P, Facchini A, Marcacci M, Buda R, Zaffagnini S, Ruggeri A. The human anterior cruciate ligament: histological and ultrastructural observations. J Anat. 1992; 180(Pt 3):515–519. [PubMed: 1487443]

35. Bashur CA, Shaffer RD, Dahlgren LA, Guelcher SA, Goldstein AS. Effect of fiber diameter and alignment of electrospun polyurethane meshes on mesenchymal progenitor cells. Tissue Eng Part A. 2009; 15(9):2435–45. [PubMed: 19292650]

36. Lyons J, Li C, Ko F. Melt-electrospinning part I: processing parameters and geometric properties. Polymer. 2004; 45(22):7597–7603.

37. Screen HR, Lee DA, Bader DL, Shelton JC. Development of a technique to determine strains in tendons using the cell nuclei. Biorheology. 2003; 40(1-3):361–8. [PubMed: 12454427]

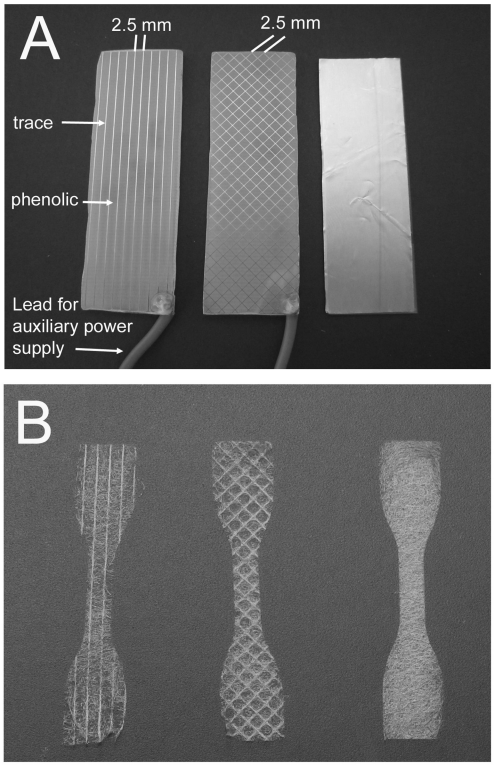

Figure 1.
Electrospinning A) templates (left to right: parallel, diamond, and unaligned), and B) scaffolds (left to right: parallel, diamond, and unaligned) with templated architecture.

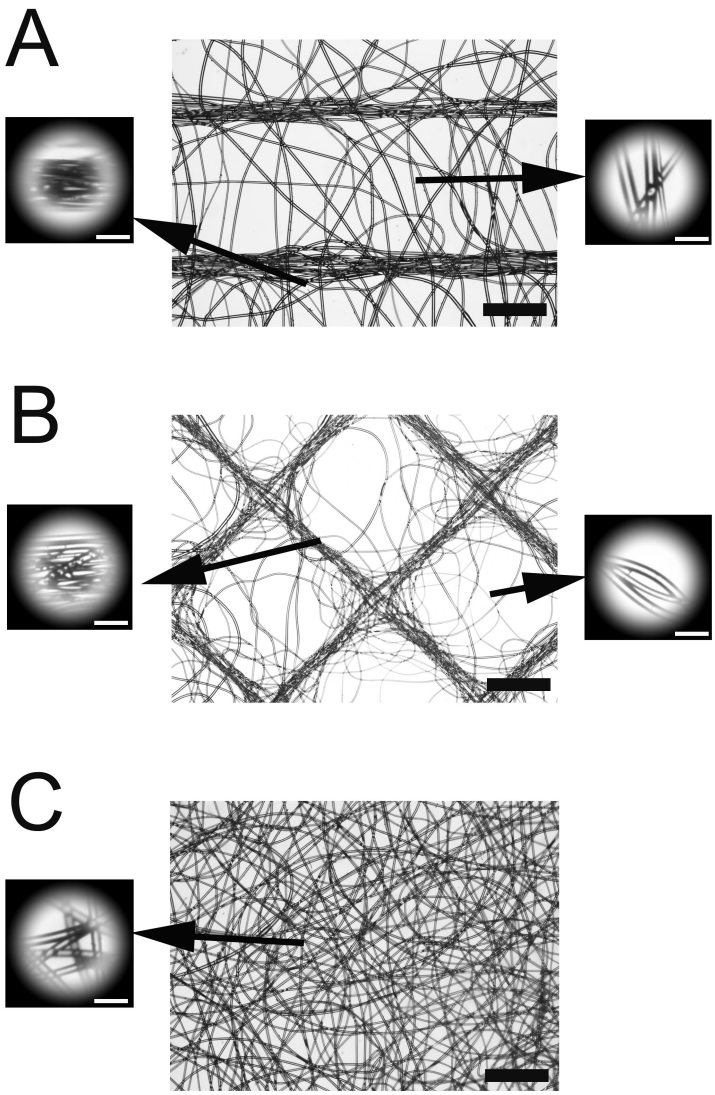

Figure 2.
Microscopy images of electrospun scaffolds: A) parallel; B) diamond; C) unaligned. Insets illustrate samples with masks taken for 2D FFT analysis. In A) samples were taken from the region midway between template traces (upper left), and on top of a trace (lower left). Similar samples were taken from B. Inset bar = 100 μm. Bar = 1 mm.

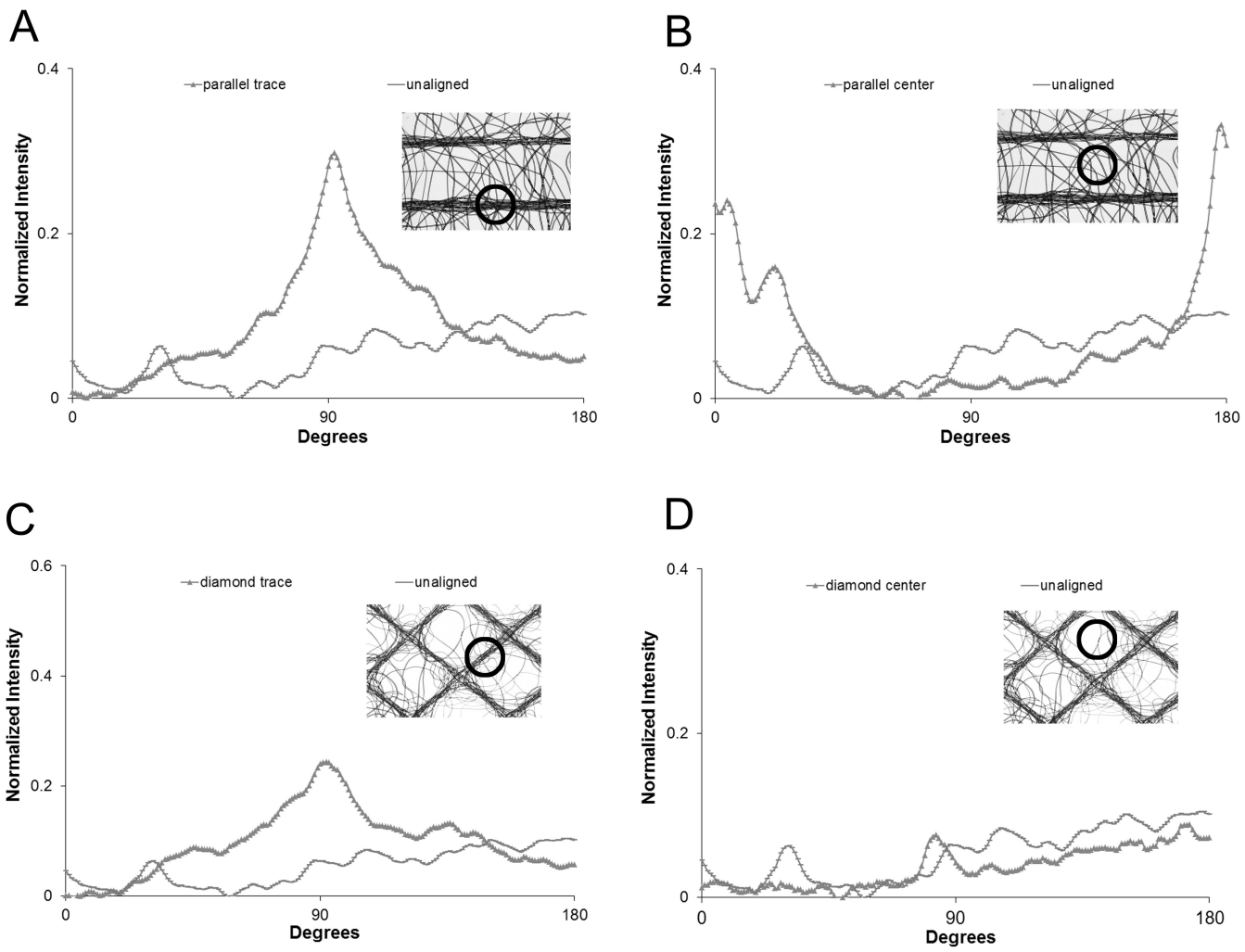

Figure 3.

Representative 2D FFT alignment plots from different locations from each scaffold: A) parallel traces; B) parallel center regions; C) diamond traces; D) diamond center regions. Insets are representative microscopy images with the locations of respective alignment plots highlighted.

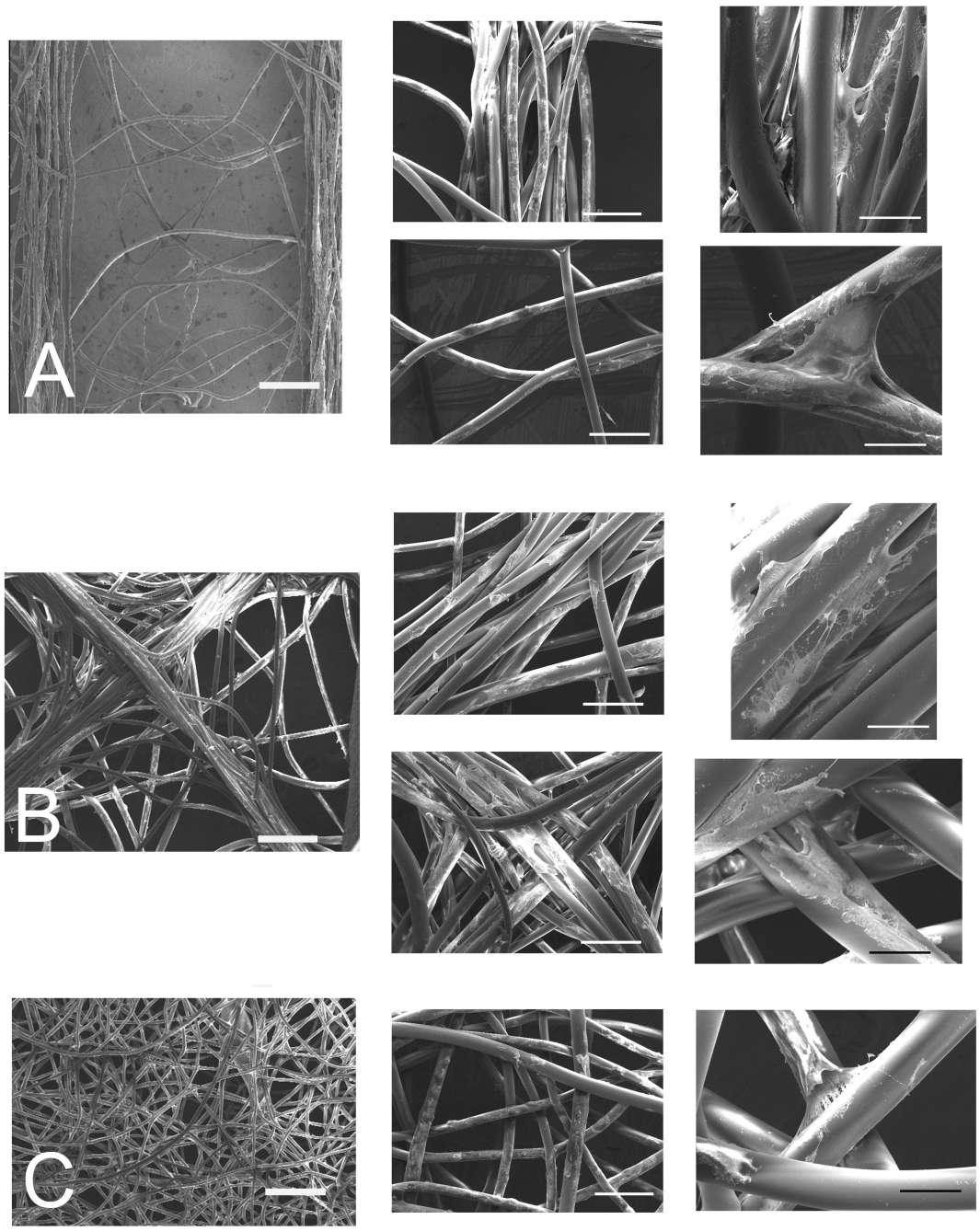

Figure 4.
SEM images of primary porcine fibroblasts on scaffolds with different fiber architecture: A) parallel, upper inset row - trace bundle, lower inset row - center region; B) diamond, upper inset row - trace bundle, lower inset row - intersection; and C) unaligned. Bars = 500 μm, 200 μm, and 50 μm from left to right.

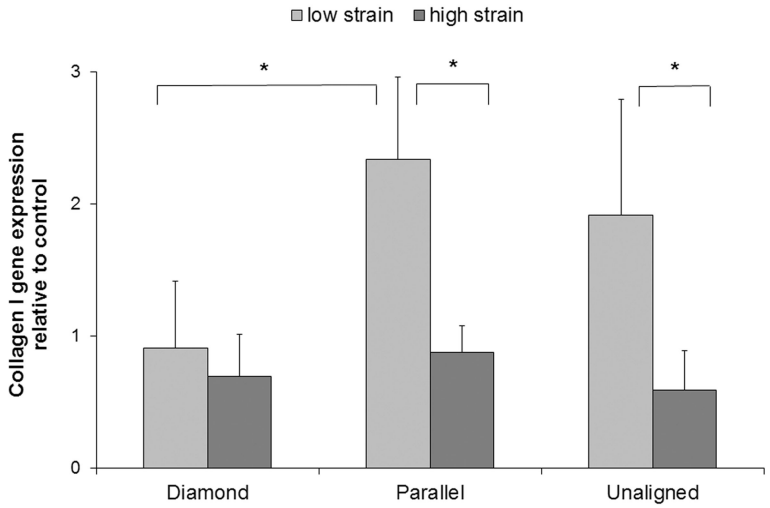

Figure 5.

Collagen I gene expression for each scaffold architecture subject to two levels of strain relative to matched unstrained controls. Data were normalized to GAPDH expression. Mean + 1 standard deviation. * indicates significance.

Table 1

Alignment ratio at each location. * indicates significance between trace and center region. + indicates significance between the specific region and the unaligned scaffold mean.

Architecture	Trace	Center Region
Parallel	8.28*,+	0.54
Diamond	6.39*,+	1.46
Unaligned	N/A	1.08

Table 2

Relevant mechanical properties for different scaffold architectures taken from two orientations. * indicates significance between 0° and 90° testing orientations within a particular template spacing. + indicates significance between the aligned and unaligned scaffolds. ˆ indicates significance between parallel and diamond scaffolds for a particular testing orientation. Significance indications are placed on the higher value.

Architecture	Orientation	Inflection Strain (%)	Ultimate Strength (MPa)	Ultimate Strain (%)
Parallel	0°	1.32	56.14*,+,ˆ	82.76+
Parallel	90°	2.69	42.94	71.23
Diamond	0°	8.45+,ˆ	43.46+	78.33
Diamond	90°	6.23+,ˆ	41.84	92.11
Unaligned	0°	1.26	28.22	52.22
Unaligned	90°	1.23	29.73	47.64

Table 3

Local strain at each nominal strain level. Mean ±1 standard deviation.

Nominal strain level	Parallel (%)	Diamond (%)	Unaligned (%)
low strain	0.9±0.0	-0.4±0.7	0.7±0.4
high strain	2.1±0.4	-0.7±1.1	2.6±0.6